clean technologies

MDPI

Article

Mercury Removal from Mining Wastewater by Phytoaccumulation in Autochthonous Aquatic Plant Species

Franco Hernan Gomez [1,2,3], Maria Cristina Collivignarelli [4,5], Ahmed Mohammad Nafea Masoud [1,2], Marco Carnevale Miino [4,*], Kelly Cristina Torres [6], Jesus Antonio Quintero [6], Sabrina Sorlini [1,2] and Mentore Vaccari [1,2,*]

1 Department of Civil, Environmental, Architectural Engineering and Mathematics, University of Brescia, Via Branze 43, 25123 Brescia, Italy
2 Research Center on Appropriate Technologies for Environmental Management in Limited Resources Countries (CeTAmb), University of Brescia, Via Branze 43, 25123 Brescia, Italy
3 Department of Chemical Engineering, Universitat Politècnica de Catalunya-BarcelonaTech, Av. Maristany 16, 08019 Barcelona, Spain
4 Department of Civil Engineering and Architecture, University of Pavia, Via Ferrata 3, 27100 Pavia, Italy
5 Interdepartmental Centre for Water Research, University of Pavia, Via Ferrata 3, 27100 Pavia, Italy
6 Research Group on Conservation and Use of Biodiversity-BioCon, Instituto Universitario de la Paz-Unipaz, km 14, vía Bucaramanga, Barrancabermeja 687033, Colombia
* Correspondence: marco.carnevalemiino01@universitadipavia.it (M.C.M.); mentore.vaccari@unibs.it (M.V.)

Abstract: Mining wastewater (MWW) can contain mercury in high concentrations. In this study, four autochthonous aquatic plant species (*Eichhornia Crassipes*—EC, *Marsilea Quadrifolia*—MQ, *Ludwigia Helminthorrhiza*—LH, and *Lemna Minor*—LM) were identified and tested for phytoaccumulation of total mercury (THg). To better study the accumulation phenomenon and macrophyte responses, this work has been divided into three phases, and pilot-scale reactors have been used to simulate real conditions. The results highlighted that, in case of 15 $\mu g_{THg,fed}$, the bioconcentration factor (BCF) was significantly higher in EC (19.04) and LH (18.41) with respect to MQ and LM (almost six times and two times higher, respectively). EC granted the best results in terms of THg accumulation (50.90%) and lower evapotranspiration of THg phenomenon with respect to LH. A significant decrease of the BCF (from 23.45 to 21.98) and an increase of the TF (from 0.23 up to 0.73) after 42 d highlighted that a breaking-time in terms of THg accumulation was reached due to the deterioration of the roots. In terms of the kinetics of THg removal by bioaccumulation, an HLT of 69.31 d was found, which is more than the breaking-time of the EC system, proving that a periodic replacement of exhausted macrophytes is required to obtain a higher percentage of THg removal.

Keywords: mercury; mining wastewater; phytoremediation; *Eichhornia Crassipes*; *Marsilea Quadrifolia*; *Ludwigia Helminthorrhiza*; *Lemna Minor*

Citation: Gomez, F.H.; Collivignarelli, M.C.; Masoud, A.M.N.; Carnevale Miino, M.; Torres, K.C.; Quintero, J.A.; Sorlini, S.; Vaccari, M. Mercury Removal from Mining Wastewater by Phytoaccumulation in Autochthonous Aquatic Plant Species. *Clean Technol.* **2023**, *5*, 839–851. https://doi.org/10.3390/cleantechnol5030041

Academic Editor: Nicolas Kalogerakis

Received: 31 December 2022
Revised: 20 January 2023
Accepted: 22 June 2023
Published: 27 June 2023

1. Introduction

Heavy metals pose a severe risk for both human and environmental health. Among the heavy metals, mercury represents a serious issue considering its persistence in the environment and its high mobility due to the strong volatility of the compounds [1]. Moreover, in humans, high doses of exposure can induce severe complications mainly to the brain and kidneys; in wildlife, mercury can (i) change biochemical process, (ii) cause damage to cells and tissues, and (iii) alter reproduction [2,3].

The presence of mercury in artisanal and small-scale gold mines (ASGM) is widespread, especially in low- middle-income countries [4,5], where extraction activities are mainly carried out with a low degree of mechanization and mercury is used for the whole-ore amalgamation process [6–8].

Although the use of mercury is the most economical way to produce gold, it produces a high environmental impact [9–11]. For instance, Oliveira et al. [12] highlighted that

amalgam residues can contain up to 450 mg_{THg} kg^{-1}, while the concentration in mining wastewater (MWW) varies from 0.5 to 3 mg_{THg} kg^{-1}. Several countries have adopted laws to limit the effect of unregulated mercury discharged into the environment. For instance, in Colombia, the current legislation banned the use of mercury in any mineral extraction activity to limit the environmental impact, envisaging a technological transition from the use of mercury in mines to the treatment of sites contaminated by mining activities [13]. However, some local authorities appealed this decision, and, at the same time, checking all ASMG can be difficult [14].

Several biological treatments have been identified to remove mercury from MWW [15–17]. However, one of the most promising and low-impact methods is phytoaccumulation, which consists of removing mercury from MWW by accumulating it in macrophytes for subsequent disposal/recovery. In this treatment, several aspects should be considered for proper management of phytoaccumulation in plants, including the concentration and characterization of contaminants to be eliminated, the age of the macrophyte, the depth of the root system, the rhizofiltration phenomenon, the impact generated by contaminated vegetation, the use of considerable surfaces, and the time required for the treatment processes [18–22].

However, not all mercury removed by the phytosystem is accumulated in macrophytes, because phytovolatilization is a well-known phenomenon that should be considered. It should also be taken into account that some studies have highlighted that mercury could re-join the aquatic environment through precipitation [22–24].

To reduce the impact of the phytoremediation process, this work focused on the use of autochthonous macrophytes as previously reported by Quintero et al. [25]. For instance, *Eichhornia Crassipes* (EC) has already been used in several studies for pollutant removal from wastewater, demonstrating its ability to accumulate in its roots mercury in concentrations 100–270 times higher than the initial one [26–28]. *Ludwigia Helminthorrhiza* (LH) has demonstrated very high performance in terms of removal capacity of mercury, with a bioconcentration factor after 27 d of treatment that reached 0.8856 μg_{THg} g^{-1} [21,29]. Furthermore, *Marsilea Quadrifolia* (MQ) has shown good potential in phytoremediation processes [30]. *Lemna Minor* (LM) is a well-known macrophyte with very good potential for heavy metal removal from wastewater, as it has been demonstrated to be able to remove 30% of mercury in 22 days [29,31–33].

In this study EC, LH, MQ, and LM have been tested for total mercury (THg) removal from MWW and accumulation, highlighting the diverse pathways of THg in the phytosystem. A three-step experimental procedure was carried out to select the best macrophyte and, for that macrophyte, the kinetic of THg removal by phytoaccumulation has been also evaluated. The results of this study will be helpful to water managers, especially in low- and middle-income countries, to optimize the treatment of Hg-polluted WW by accumulation in aquatic macrophytes.

2. Materials and Methods

2.1. Characteristics of Mining Wastewater

MWW was collected from a sampling site in the northern part of Colombia. The total mercury (THg) concentration in samples was 488 μg_{THg} L^{-1}, and lower concentrations were obtained with proper dilutions of the MWW. COD and BOD_5 were 617 mg L^{-1} and 365 mg L^{-1}, respectively. Phosphorus was also detected, and its concentration was 1.27 mg L^{-1}.

2.2. Pilot-Scale Systems

Three diverse types of pilot-scale systems (PSSs) were used depending on the phase of the tests (Figure 1).

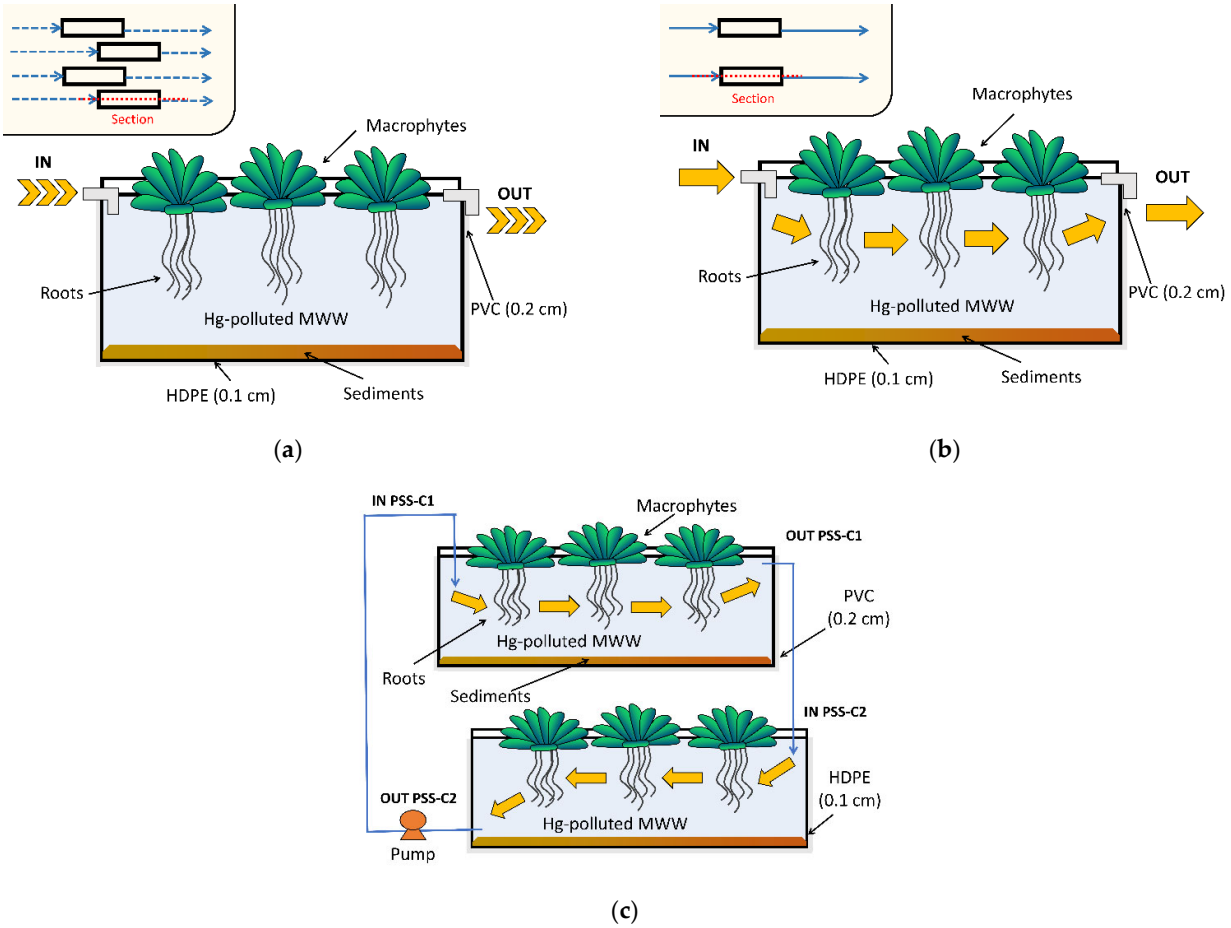

Figure 1. Characteristics of the reactors used in (**a**) PSS-A, (**b**) PSS-B, and (**c**) PSS-C.

PSS-A was made of four reactors in parallel (volume: 5 L for each). In each reactor, a diverse type of macrophyte was located (EC, MQ, LH, and LM) (Figure 1a). PSS-B was composed of two reactors in parallel (volume: 5 L for each), and in each reactor was located one of the two best macrophytes selected from the previous phase (Figure 1b). Finally, PSS-C was composed of two reactors (volume: 50 L for each) operating in series thanks to a pump system, which recirculated the treated MWW extracted from the PSS-C2 into PSS-C1 (Figure 1c).

Each reactor was made of polyvinyl chloride (PVC) (thickness: 0.2 cm) and was waterproofed with a layer (0.1 cm) of high-density polyethylene (HDPE). The inlet and outlet pipes (1.1 cm internal diameter) were made of PVC. The reactors were equipped to be illuminated by means of lamps (15 W nominal power) for 12 h a day in order to promote chlorophyll photosynthesis.

Before starting the tests, it was checked that in all reactors, the leaf system covered almost all of the available area, and that the roots of the macrophytes were long enough to also reach the sediments at the bottom of the reactor.

2.3. Experimental Design and Management Mode

Three diverse phases were carried out with different aims.

Phase A (Ph-A) was carried out using PSS-A operating in batch mode. This phase aimed to compare the efficiency of EC, MQ, LH, and LM in bioaccumulating THg, which would allow for the selection of the two best macrophytes. Moreover, the influence of the initial THg concentration in MWW on the bioaccumulation phenomenon was evaluated. Properly diluted (3 μg_{THg} L^{-1}, 42 μg_{THg} L^{-1}, and 488 μg_{THg} L^{-1}) MWW was fed to the reactor (t = 0), and after 27 d, samples of macrophytes, sediments, and water were taken.

The two best macrophytes selected from Ph-A were tested in phase B (Ph-B) by means of PSS-B to verify the bioaccumulation capacity operating in continuous mode for 14 days. MWW (THg: 210 μg_{THg} L^{-1}) with a flowrate of 2 L d^{-1} was fed continuously with a hydraulic retention time (HRT) of almost 20 min.

In phase C (Ph-C), the optimal macrophyte selected based on the results of Ph-B was used in PSS-C for testing the bioaccumulation phenomenon in the case of a longer HRT (56 d). This phase also had the aim of evaluating the breaking-time in terms of plant deterioration. Reactors in PSS-C operated in semi-batch mode, and a high recirculation of MWW in the system was maintained (0.5 L s^{-1}) to limit THg sedimentation.

2.4. Balance of Total Mercury in the Systems

During tests, the mass balance of mercury in the phytosystem was calculated considering four diverse THg pathways: (i) bioaccumulation in macrophytes, (ii) evapotranspiration in the atmosphere, and residual concentration (iii) in treated effluent and (iv) in sediments (Figure 2).

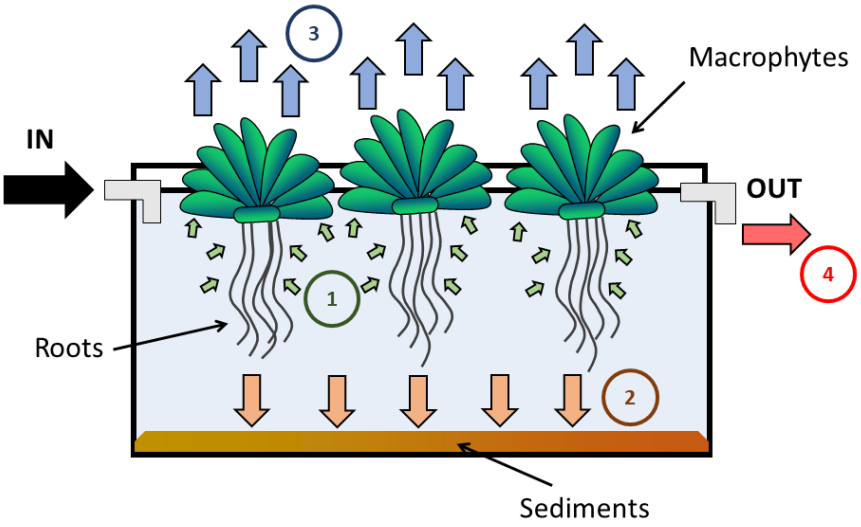

Figure 2. Scheme of the pathways assumed in the phytosystem, where 1 = accumulation in the macrophyte; 2 = sedimentation; 3 = evapotranspiration; 4 = outlet the system in treated wastewater.

The THg concentration was measured in the MWW fed, the macrophytes' tissues, the sediments, and the treated wastewater outlet system. The amount of THg subjected to evapotranspiration was calculated as reported in Equation (1):

$$ET\ (\mu g) = IN - ACC - SED - OUT, \quad (1)$$

where IN and OUT are the amount of THg fed and extracted from the system (µg), respectively. ACC refers to THg accumulated by the macrophyte (µg), while SED is the amount of mercury deposited in the reactor (µg).

2.5. Bioconcentration and Translocation Factors

The bioconcentration factor (BCF) in the macrophytes was calculated based on THg concentration in plant tissues, considering both the aerial part and the roots, according to Equation (2) [34–36]:

$$BCF\ (-) = (C_{f,m} - C_{0,m})\ C_a{}^{-1}, \quad (2)$$

where $C_{0,m}$ and $C_{f,m}$ represent the concentration of THg in the macrophytes at the initial time and after contamination exposure (µg kg^{-1}), respectively, and C_a is the concentration of THg in WW fed to the system (µg L^{-1}).

In Ph-C, the translocation factor (TF) was also evaluated according to Equation (3) [36]:

$$TF\ (-) = C_l\ C_r{}^{-1}, \quad (3)$$

where C_l and C_r represent the concentration of THg in unsubmerged parts (e.g., leaves) and in roots ($\mu g\ kg^{-1}$), respectively.

2.6. Kinetic of THg Removal by Phytoaccumulation

In Ph-C, the kinetic of THg removal by phytoaccumulation was calculated. Assuming PSS-C operated according to a plug flow behavior, THg removal was assumed to follow a pseudo-first order removal model [37–39] using the following equations (Equations (4) and (5)) [40,41]:

$$\ln(THg_i\ THg_{fed}{}^{-1}) = -k \times t, \quad (4)$$

$$HLT = \ln(2)\ k^{-1}, \quad (5)$$

where THg_{fed} represents the amount of THg fed to the system (μg) while THg_i indicates the not-already-phyto-accumulated THg (μg) at time t (d). k represents the first-order kinetic constant of the reaction (d^{-1}) while HLT is the half-lifetime of the pollutant (d).

2.7. Analytical Methods

THg was measured both in aqueous and solid samples by the mercury analyzer RA-915M equipped with RP-92 Cold Vapor for aqueous samples and the PYRO-915+ pyrolysis attachment for testing solid samples.

3. Results and Discussion

3.1. Phase A

EC, MQ, LH, and LM were monitored in terms of their root and aerial structures (stems and leaves).

EC showed good adaptability to an environment contaminated by varying concentrations of mercury. The plant showed very good adaptation to the conditions of the experiment, and it did not show any problems with decay or deterioration of the roots, stem, or leaves (Figure 3a).

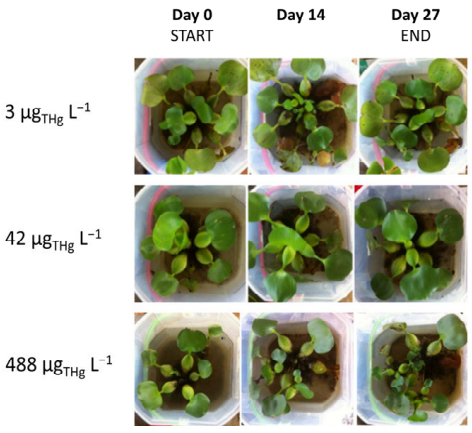

(**a**)

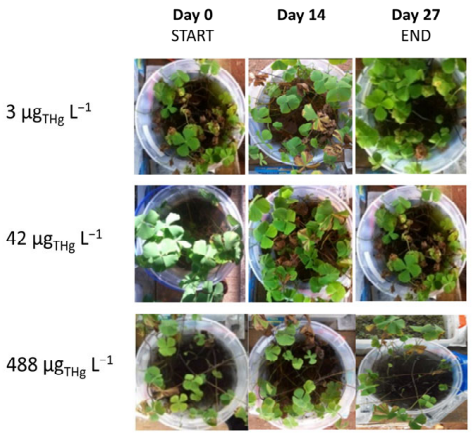

(**b**)

Figure 3. *Cont.*

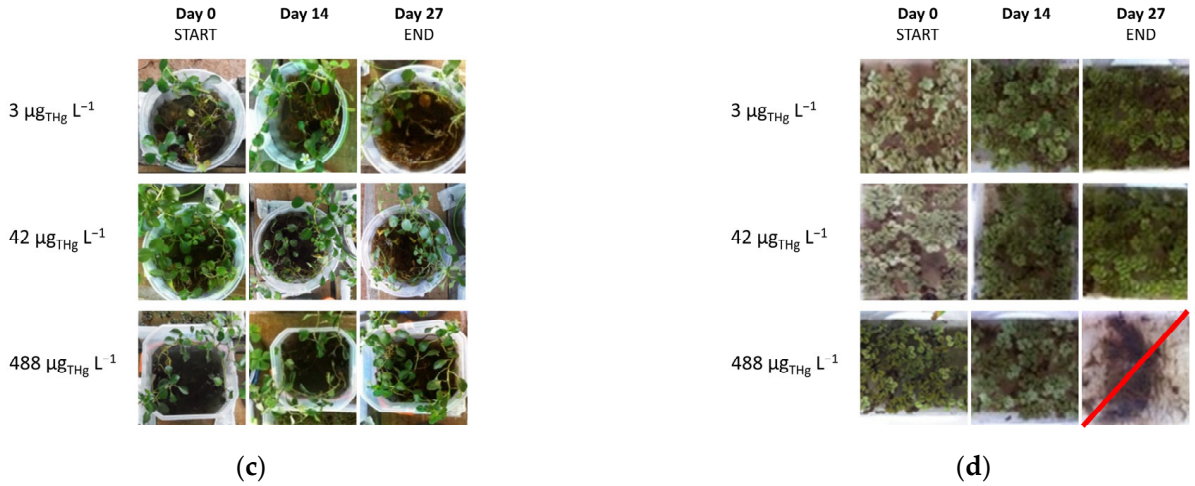

Figure 3. Effect of initial THg concentration on the aerial parts of the macrophytes for (**a**) EC, (**b**) MQ, (**c**) LH, and (**d**) LM, from day 0 to day 27.

MQ showed the phenomenon of tissue deterioration in both the root and aerial parts, but overall, it was able to adapt and survived until the end of the test (Figure 3b). It showed dual behavior: high reproductive capacity characterized by new shoot growth contrasted with the necrosis of many plant tissues.

LH developed rapidly, producing inflorescences and growing new spongy rhizomes necessary for floating the stems on the water surface. Good adaptability, with no deterioration of root or aerial plant tissues, was observed (Figure 3c).

LM did not perform well in terms of vegetative development, highlighting some problems in adaptation to high THg concentrations (Figure 3d). Changes in the color of the leaves, fragility of the tissues, and lacerations were observed, confirming previous results [31,33]. For these reasons, LM did not withstand the maximum concentration of 488 μg$_{THg}$ L^{-1}.

Considering THg accumulation in the plant systems, the higher the amount of THg fed, the higher the amount of THg accumulated (Figure 4a). The stronger influence of the amount of THg fed on the accumulation phenomenon was highlighted with LH (47.84 mg$_{THg}$ kg$_{DW}^{-1}$ mg$_{fed}^{-1}$) and EC (43.48 mg$_{THg}$ kg$_{DW}^{-1}$ mg$_{fed}^{-1}$). LM allowed for the accumulation of only 23.65 mg$_{THg}$ kg$_{DW}^{-1}$ mg$_{fed}^{-1}$ of THg fed, while a lower result was reached using MQ (6.69 mg$_{THg}$ kg$_{DW}^{-1}$ mg$_{fed}^{-1}$).

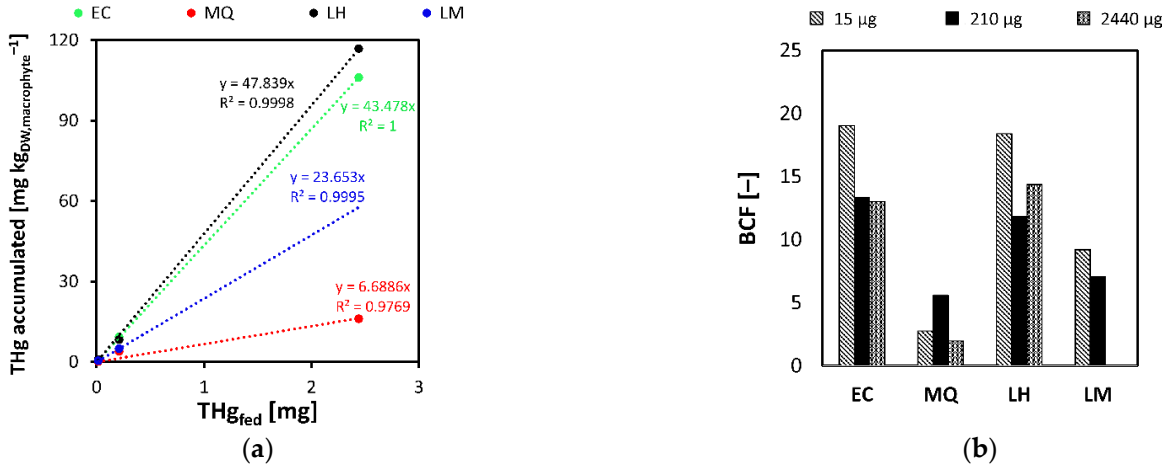

Figure 4. (**a**) THg accumulated in macrophytes as a function of TH$_{fed}$ and (**b**) BCF after 27 d as a function of the type of macrophyte and THg$_{fed}$.

The BCF was calculated after 27 d as a function of the type of macrophyte and the amount of initial THg_{fed}. The results highlighted that the BCF was significantly higher in EC and LH with respect to MQ and LM. Up to 19.04 and 18.41 were calculated for EC and LH, respectively, in the case of 15 $\mu g_{THg,fed}$. These values were almost two times and six times higher than the BCF of LM and MQ, respectively, in the same conditions. Considering the higher initial THg fed (2440 $\mu g_{THg,fed}$), the BCF remained stronger in the case of EC and LH (13.04 and 14.37, respectively) compared to other macrophytes. Considering also that EC and LH demonstrated optimal growth without adaptive problems at high concentrations of THg, it can be stated that these two macrophytes present the best response.

A balance of THg in the system after 27 d as a function of the type of macrophyte and the amount of initial THg_{fed} was evaluated (Figure 5). In agreement with BCF values and considering all tested initial pollutant concentrations, higher THg accumulation was founded in macrophytes EC (30.29 ± 6.23%) and LH (29.76 ± 6.11%). Considering the total amount of THg removed (through accumulation and evapotranspiration), MQ reached the highest values (80.3 ± 7.42%) but with evapotranspiration losses more than ten times the THg accumulated (73.41 ± 6.82% vs. 6.89 ± 3.51%).

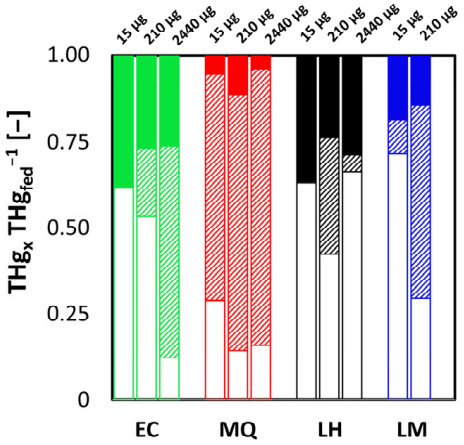

Figure 5. Balance of the THg in the different phases of the system (THg_x) as a function of the type of macrophyte and THg_{fed}. The solid columns refer to the THg accumulated in the roots and in the aerial parts of the macrophytes (THg_x); the striped columns indicate the amount of THg evapotranspirated; the white columns refer to the THg not removed (settled or in the MWW after treatment). (Duration: 27 d).

This result is due to the different types of mechanisms of phytoremediation. In the case of LH and EC, THg is absorbed by the roots and is either precipitated within the root zone or migrates to all parts of the plant (e.g., shoots and leaves). Mercury removed from polluted water is accumulated in the phytosystem to prevent its movement [24,42]. Some studies also suggest that accumulated THg could also be transformed into less toxic compounds thanks to redox reactions [43]. Based on our results, THg in MQ followed another mechanism of removal. Mercury is absorbed by the plants and transformed into less toxic contaminants (e.g., dimethyl selenide and mercuric oxide) and then released into the atmosphere through the evapotranspiration process [24,42]. Some studies have pointed out that in this case, mercury can re-join the aquatic environment through precipitation [24].

Higher percentages of THg in sediments and treated water were highlighted in the case of LH (57.33 ± 12.06%) and LM (50.55 ± 29.14%). However, in the case of LH, almost double the percentage of THg accumulated was found with respect to LM (16.30 ± 2.95%).

Considering the results of the tests in Ph-A, EC and LH were selected for Ph-B.

3.2. Phase B

In continuous-flow conditions, good results obtained in batch tests (Ph-A) in terms of THg accumulation by EC and LH were confirmed. EC reached the highest BCF (16.80)

and THg accumulated (58.80 mg_{THg} kg_{DW}^{-1} mg_{fed}^{-1}) with respect to LH (14.84 and 51.89 mg_{THg} kg_{DW}^{-1} mg_{fed}^{-1}, respectively) (Figure 6a). This result can be explained by the stronger vegetative development found during the monitoring of EC with respect to LH, where progressive leaf thinning was recorded (Figure A1). EC maintained a high growth capacity, which led it to colonize the entire available surface area.

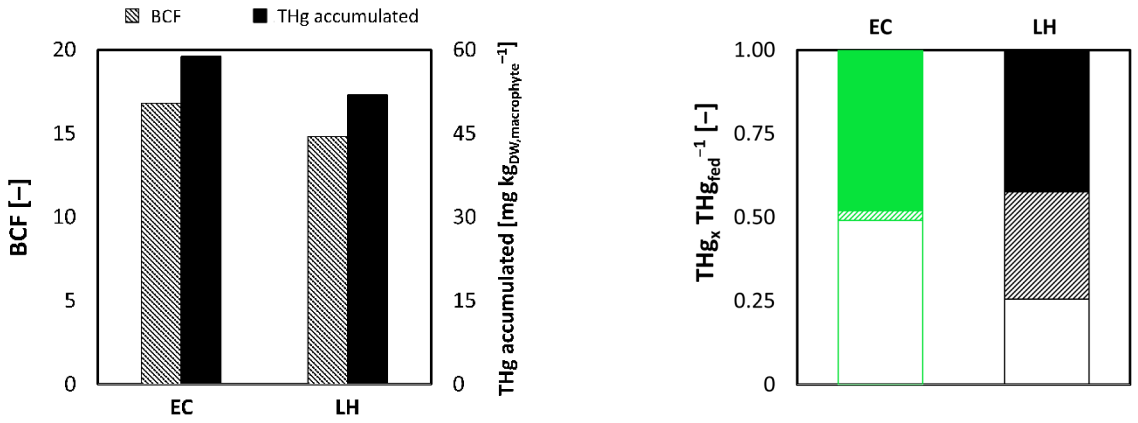

(**a**) (**b**)

Figure 6. (**a**) BCF and THg accumulated in macrophytes as a function of the type of macrophyte. (**b**) Balance of the THg in the different phases of the system (THg_x) as a function of the type of macrophyte. The solid columns refer to the THg accumulated in the roots and in the aerial parts of the macrophytes; the striped columns indicate the amount of THg evapotranspirated; the white columns refer to the THg not removed (settled or in the MWW after treatment). (Initial concentration = 210 μg_{THg} L^{-1}, flowrate = 2 L d^{-1}, duration = 14 d).

LH granted the best results in terms of THg removal (74.44%) but the lowest in terms of THg accumulation (42.36%) with respect to EC (50.90% and 48%, respectively) due to a higher evapotranspiration phenomenon estimated in LH with respect to EC (32.08% vs. 2.90%, respectively) (Figure 6b). This phenomenon should be further investigated because it represents a key aspect of trying to reduce the toxicological impact of evapotranspiration [22,28,44]. In previous studies, in the case of other heavy metals (e.g., chromium), EC has shown better performance than *Ludwigia* sp. in bioaccumulating the pollutant [45].

Considering the results of the tests in Ph-B, EC was selected for Ph-C.

3.3. Phase C

This phase was tested to evaluate the BCF and the TF as functions of the contact time and to highlight the breaking-time in terms of THg accumulation by EC.

The results showed a progressive increase in the BCF considering both the roots and the aerial parts of the macrophytes (Figure 7). The highest value of the BCF was reached on day 42 (23.45), while on day 56, a reduction of the BCF was highlighted (21.98). Therefore, the results proved that the breaking-time in terms of THg accumulation by EC was after 6 weeks. After this period, the macrophytes (in particular, the roots) deteriorated, and the concentration of mercury in the tissues decreased according to Mishra et al. [31].

This aspect is made clearer by studying the evolution of the TF during the test (Figure 7). The behavior was similar to the BCF with an increase up to 0.23 on day 42. This means that THg was mainly accumulated in the roots instead of other non-submerged tissues, in accordance with Skinner et al. [22]. Furthermore, Pelcová et al. [46] highlighted that EC roots have a high potential for Hg accumulation with concentrations 10–21 times higher than in leaves depending on environmental conditions. The accumulation of Hg is higher in roots due their direct contact with polluted WW (as EC is a floating macrophyte), while in case of submerged plants, a marked difference between the roots and the leaves is generally not visible [46]. However, after breaking-time, the TF significantly increased up

to 0.73, despite the reduction of the BCF. This result is directly linked to the deterioration of the roots of EC after long exposure to heavy THg-polluted waters. The amount of THg accumulated in the roots decreased, increasing the TF but decreasing the BCF.

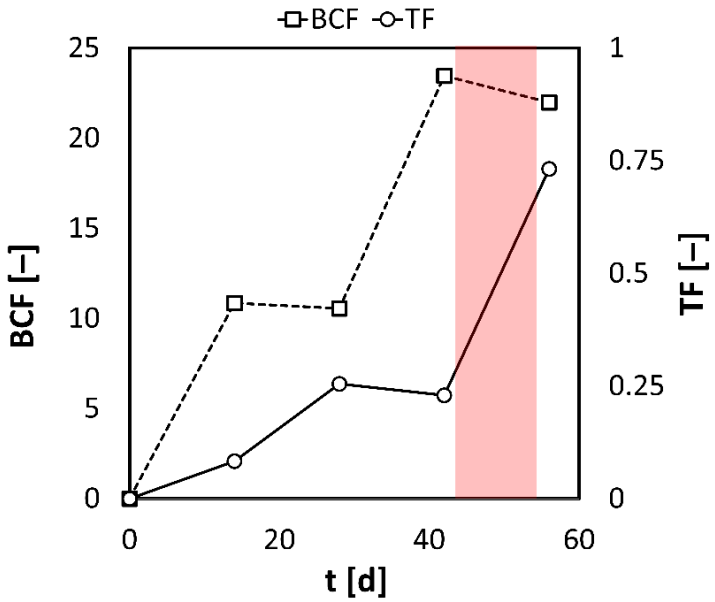

Figure 7. BCF and TF as a function of the contact time for EC. The red band highlights the breaking-time. (Initial concentration = 286 μg_{THg} L^{-1}, flowrate = 0.5 L s^{-1}).

Moreover, the experimental pseudo-first order kinetic constant (k) of THg removal by accumulation in EC was calculated (Figure 8). Considering only the first 42 days of the test, in which the breaking-time was not reached, the pseudo-first order kinetic constant (k) was evaluated as 0.01 d^{-1}. This results in an HLT equal to 69.31 d, which is more than the breaking-time of the EC system.

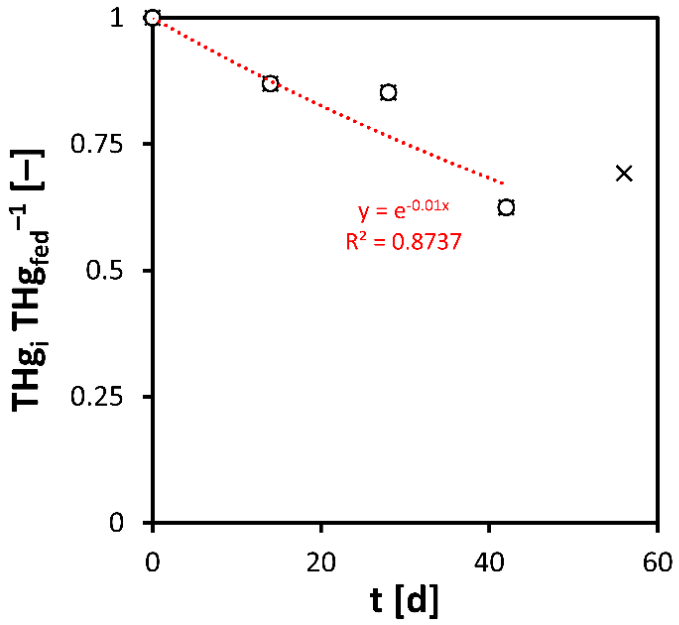

Figure 8. THg removal by accumulation in EC according to a pseudo-first order kinetic model. Data after breaking-time, indicated by X, have been excluded. (Initial concentration = 286 μg_{THg} L^{-1}, flowrate = 0.5 L s^{-1}).

Therefore, this bio-treatment can be very useful for removing THg from water by bioaccumulating it in macrophytes. However, without a periodic replacement of exhausted macrophytes, a very high percentage of pollutant removal cannot be reached due to the significant time required, which is longer than the breaking-time of the system in terms of THg accumulation.

4. Conclusions

EC, MQ, LH, and LM have been tested for phytoaccumulation of mercury present in MWW. This work has been divided into three phases to better select the optimal macrophyte to maximize THg accumulation. The stronger influence of the amount of THg fed on the accumulation phenomenon was highlighted with LH (47.84 $mg_{THg}\ kg_{DW}{}^{-1}\ mg_{fed}{}^{-1}$) and EC (43.48 $mg_{THg}\ kg_{DW}{}^{-1}\ mg_{fed}{}^{-1}$). LM accumulated only 23.65 $mg_{THg}\ kg_{DW}{}^{-1}\ mg_{fed}{}^{-1}$ of the THg fed, while a lower result was reached using MQ (6.69 $mg_{THg}\ kg_{DW}{}^{-1}\ mg_{fed}{}^{-1}$). The results highlighted that the BCF was significantly higher in EC and LH with respect to MQ and LM (almost six times and two times, respectively). Among LH and EC, LH granted the best results in terms of THg removal, but the lowest in terms of THg accumulation with respect to EC (42.36% vs. 50.90%, respectively) due to a higher evapotranspiration phenomenon. EC was demonstrated to be the optimal macrophyte with the highest value of the BCF reached on day 42 (23.45). This study also highlighted that breaking-time in terms of THg accumulation by EC was after 6 weeks due to the deterioration of the roots, proved by a significant increase of the TF (from 0.23 up to 0.73). In terms of the kinetics of THg removal by bioaccumulation, k and HLT equal to 0.01 d^{-1} and 69.31 d were found, which were more than the breaking-time of the EC system. These results highlighted that the treatment of highly THg-polluted WW by phytoaccumulation in EC is possible only with a periodic replacement of the exhausted macrophyte. This work can be useful, especially in low- and middle-income countries, for optimizing the treatment of Hg-polluted WW by low-cost treatments, such as accumulation in aquatic macrophytes.

Author Contributions: Conceptualization, F.H.G., K.C.T., J.A.Q., S.S. and M.V.; methodology, F.H.G., K.C.T., J.A.Q. and S.S.; validation, K.C.T., J.A.Q., S.S. and M.V.; formal analysis, F.H.G., M.C.M. and S.S.; investigation, F.H.G. and J.A.Q.; resources, K.C.T., J.A.Q., S.S. and M.V.; data curation, F.H.G., M.C.C., M.C.M. and A.M.N.M.; writing—original draft preparation, F.H.G., A.M.N.M., S.S. and M.V.; writing—review and editing, M.C.C. and M.C.M.; visualization, F.H.G., A.M.N.M. and M.C.C.; supervision, K.C.T., J.A.Q., S.S. and M.V.; project administration, K.C.T., J.A.Q., S.S. and M.V.; funding acquisition, K.C.T., J.A.Q., S.S. and M.V. All authors have read and agreed to the published version of the manuscript.

Funding: This research received no external funding.

Institutional Review Board Statement: Not applicable.

Informed Consent Statement: Not applicable.

Data Availability Statement: All data generated or analyzed during this study are included in this published article.

Acknowledgments: This research has been developed within the academic collaboration agreement between the CeTAmb—Research Center on Appropriate Technologies for Environmental Management in Limited Resources Countries of the University of Brescia (Italy), the UNIPAZ—Instituto Universitario de la Paz (Colombia), and the Peasant Association of the Cimitarra River Valley ACVC (Colombia). The authors would also like to thank the Universidad Industrial de Santander (Bucaramanga, Colombia) for the analysis of THg both in aqueous and solid samples.

Conflicts of Interest: The authors declare no conflict of interest.

Appendix A

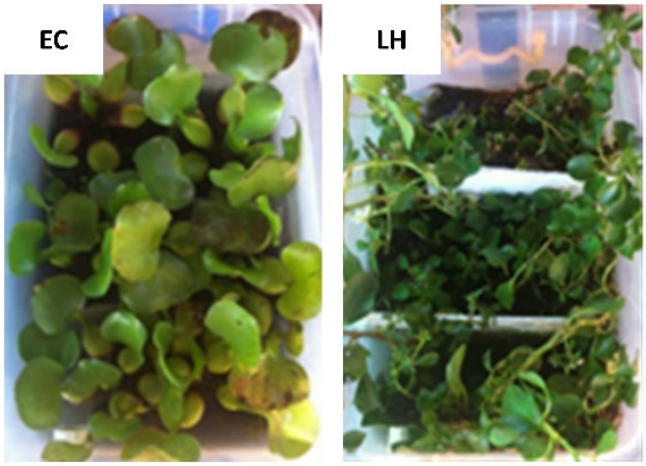

Figure A1. Macrophytes in Ph-B after 14 d.

References

1. Gworek, B.; Dmuchowski, W.; Baczewska-Dąbrowska, A.H. Mercury in the Terrestrial Environment: A Review. *Environ. Sci. Eur.* **2020**, *32*, 128. [CrossRef]
2. Park, J.-D.; Zheng, W. Human Exposure and Health Effects of Inorganic and Elemental Mercury. *J. Prev. Med. Public Health* **2012**, *45*, 344–352. [CrossRef] [PubMed]
3. Driscoll, C.T.; Mason, R.P.; Chan, H.M.; Jacob, D.J.; Pirrone, N. Mercury as a Global Pollutant: Sources, Pathways, and Effects. *Environ. Sci. Technol.* **2013**, *47*, 4967–4983. [CrossRef] [PubMed]
4. UNEP. *Sound Tailings Management in Artisanal and Small-Scale Gold Mining—Technical Document*; United Nations Environment Programme: Geneva, Switzerland, 2021.
5. World Bank. *State of the Artisanal and Small-Scale Mining Sector*; World Bank: Washington, DC, USA, 2019.
6. Yoshimura, A.; Suemasu, K.; Veiga, M.M. Estimation of Mercury Losses and Gold Production by Artisanal and Small-Scale Gold Mining (ASGM). *J. Sustain. Metall.* **2021**, *7*, 1045–1059. [CrossRef]
7. Seccatore, J.; Veiga, M.; Origliasso, C.; Marin, T.; de Tomi, G. An Estimation of the Artisanal Small-Scale Production of Gold in the World. *Sci. Total Environ.* **2014**, *496*, 662–667. [CrossRef] [PubMed]
8. Cuya, A.; Glikman, J.A.; Groenendijk, J.; Macdonald, D.W.; Swaisgood, R.R.; Barocas, A. Socio-Environmental Perceptions and Barriers to Conservation Engagement among Artisanal Small-Scale Gold Mining Communities in Southeastern Peru. *Glob. Ecol. Conserv.* **2021**, *31*, e01816. [CrossRef]
9. Telmer, K.H.; Veiga, M.M. *World Emissions of Mercury from Artisanal and Small Scale Gold Mining and the Knowledge Gaps about Them*; World Bank: New York, NY, USA, 2008.
10. Cordy, P.; Veiga, M.M.; Salih, I.; Al-Saadi, S.; Console, S.; Garcia, O.; Mesa, L.A.; Velásquez-López, P.C.; Roeser, M. Mercury Contamination from Artisanal Gold Mining in Antioquia, Colombia: The World's Highest per Capita Mercury Pollution. *Sci. Total Environ.* **2011**, *410–411*, 154–160. [CrossRef]
11. Aghaei, E.; Alorro, R.D.; Tadesse, B.; Browner, R. A Review on Current Practices and Emerging Technologies for Sustainable Management, Sequestration and Stabilization of Mercury from Gold Processing Streams. *J. Environ. Manag.* **2019**, *249*, 109367. [CrossRef]
12. Oliveira, L.J.; Hylander, L.D.; e Silva, E.d.C. Mercury Behavior in a Tropical Environment: The Case of Small-Scale Gold Mining in Poconé, Brazil. *Environ. Pract.* **2004**, *6*, 121–134. [CrossRef]
13. República de Colombia. *Resolución n. N. 1658/2013—By Means of Which Provisions Are Established for the Marketing and Use of Mercury in the Different Industrial Activities of the Country, Requirements and Incentives Are Established for Its Reduction and Elimination and Other Provisions Are Given*; Congreso de la República de Colombia: Bogotá, Colombia, 2013. (In Spanish)
14. Vélez-Torres, I.; Vanegas, D. Contentious Environmental Governance in Polluted Gold Mining Geographies: The Case of La Toma, Colombia. *World Dev.* **2022**, *157*, 105953. [CrossRef]
15. Su, Y.; Han, F.X.; Chen, J.; Sridhar, B.B.M.; Monts, D.L. Phytoextraction and Accumulation of Mercury in Three Plant Species: Indian Mustard (*Brassica juncea*), Beard Grass (*Polypogon monospeliensis*), and Chinese Brake Fern (*Pteris vittata*). *Int. J. Phytoremediation* **2008**, *10*, 547–560. [CrossRef]
16. Zolnikov, T.R.; Ramirez Ortiz, D. A Systematic Review on the Management and Treatment of Mercury in Artisanal Gold Mining. *Sci. Total Environ.* **2018**, *633*, 816–824. [CrossRef]
17. Wang, J.; Feng, X.; Anderson, C.W.N.; Xing, Y.; Shang, L. Remediation of Mercury Contaminated Sites—A Review. *J. Hazard. Mater.* **2012**, *221–222*, 1–18. [CrossRef]

18. Tangahu, B.V.; Sheikh Abdullah, S.R.; Basri, H.; Idris, M.; Anuar, N.; Mukhlisin, M. A Review on Heavy Metals (As, Pb, and Hg) Uptake by Plants through Phytoremediation. *Int. J. Chem. Eng.* **2011**, *2011*, 939161. [CrossRef]
19. Brumbaugh, W.G.; Krabbenhoft, D.P.; Helsel, D.R.; Wiener, J.G.; Echols, K.R. *A National Pilot Study of Mercury Contamination of Aquatic Ecosystems Along Multiple Gradients: Bioaccumulation in Fish (No. 2001-0009)*; U.S. Fish and Wildlife Service: Arlington, VA, USA, 2001.
20. Willis, J.M.; Gambrell, R.P.; Hester, M.W. Growth Response and Tissue Accumulation Trends of Herbaceous Wetland Plant Species Exposed to Elevated Aqueous Mercury Levels. *Int. J. Phytoremediation* **2010**, *12*, 586–598. [CrossRef] [PubMed]
21. Núñez, S.E.R.; Negrete, J.L.M.; Rios, J.E.A.; Hadad, H.R.; Maine, M.A. Hg, Cu, Pb, Cd, and Zn Accumulation in Macrophytes Growing in Tropical Wetlands. *Water Air Soil Pollut.* **2011**, *216*, 361–373. [CrossRef]
22. Skinner, K.; Wright, N.; Porter-Goff, E. Mercury Uptake and Accumulation by Four Species of Aquatic Plants. *Environ. Pollut.* **2007**, *145*, 234–237. [CrossRef] [PubMed]
23. Moreno, F.N.; Anderson, C.W.N.; Stewart, R.B.; Robinson, B.H. Phytofiltration of Mercury-Contaminated Water: Volatilisation and Plant-Accumulation Aspects. *Env. Exp. Bot.* **2008**, *62*, 78–85. [CrossRef]
24. Jeevanantham, S.; Saravanan, A.; Hemavathy, R.V.; Kumar, P.S.; Yaashikaa, P.R.; Yuvaraj, D. Removal of Toxic Pollutants from Water Environment by Phytoremediation: A Survey on Application and Future Prospects. *Environ. Technol. Innov.* **2019**, *13*, 264–276. [CrossRef]
25. Quintero, J.A.; Porras, O.O.; Torres, K.C. *Plantas Acuáticas—Magdalena Medio Colombiano*; Instituto Universitario de la Paz—Dirección de Investigación y Proyección Social: Barrancabermeja, Colombia, 2020; Volume 1.
26. Carrión, C.; Ponce-de León, C.; Cram, S.; Sommer, I.; Hernández, M.; Vanegas, C. Potential Use of Water Hyacinth (*Eichhornia crassipes*) in Xochimilco for Metal Phytoremediation. *Agrociencia* **2012**, *46*, 609–620.
27. Carvalho Dos Santos, M.; Lenzi, E. The Use of Aquatic Macrophytes (*Eichhornia crassipes*) as a Biological Filter in the Treatment of Lead Contaminated Effluents. *Environ. Technol.* **2000**, *21*, 615–622. [CrossRef]
28. Moreno, F.N.; Anderson, C.W.N.; Stewart, R.B.; Robinson, B.H. Mercury Volatilisation and Phytoextraction from Base-Metal Mine Tailings. *Environ. Pollut.* **2005**, *136*, 341–352. [CrossRef] [PubMed]
29. Kamal, M. Phytoaccumulation of Heavy Metals by Aquatic Plants. *Environ. Int.* **2004**, *29*, 1029–1039. [CrossRef]
30. Abbasi, S.A.; Ponni, G.; Tauseef, S.M. Marsilea Quadrifolia: A New Bioagent for Treating Wastewater. *Water Air Soil Pollut.* **2018**, *229*, 133. [CrossRef]
31. Mishra, V.K.; Upadhyay, A.R.; Pathak, V.; Tripathi, B.D. Phytoremediation of Mercury and Arsenic from Tropical Opencast Coalmine Effluent Through Naturally Occurring Aquatic Macrophytes. *Water Air Soil Pollut.* **2008**, *192*, 303–314. [CrossRef]
32. Arenas, A.D.; Marcó, L.M.; Torres, G. Evaluación de La Planta Lemna Minor Como Biorremediadora de Aguas Contaminadas Con Mercurio. *Av. Cienc. Ing.* **2011**, *2*, 1–11.
33. Ekperusi, A.O.; Sikoki, F.D.; Nwachukwu, E.O. Application of Common Duckweed (*Lemna minor*) in Phytoremediation of Chemicals in the Environment: State and Future Perspective. *Chemosphere* **2019**, *223*, 285–309. [CrossRef]
34. Jayampathi, T.; Atugoda, T.; Jayasinghe, C. Uptake and Accumulation of Pharmaceuticals and Personal Care Products in Leafy Vegetables. In *Pharmaceuticals and Personal Care Products: Waste Management and Treatment Technology*; Elsevier: Amsterdam, The Netherlands, 2019; pp. 87–113.
35. Wang, W.-X. Bioaccumulation and Biomonitoring. In *Marine Ecotoxicology*; Elsevier: Amsterdam, The Netherlands, 2016; pp. 99–119.
36. Mishra, T.; Pandey, V.C. Phytoremediation of Red Mud Deposits Through Natural Succession. In *Phytomanagement of Polluted Sites*; Elsevier: Amsterdam, The Netherlands, 2019; pp. 409–424.
37. Panja, S.; Sarkar, D.; Zhang, Z.; Datta, R. Removal of Antibiotics and Nutrients by Vetiver Grass (Chrysopogon Zizanioides) from a Plug Flow Reactor Based Constructed Wetland Model. *Toxics* **2021**, *9*, 84. [CrossRef]
38. Dombeck, G.D.; Perry, M.W.; Phinney, J.T. Mass Balance on Water Column Trace Metals in a Free-Surface-Flow-Constructed Wetlands in Sacramento, California. *Ecol. Eng.* **1998**, *10*, 313–339. [CrossRef]
39. Von Sperling, M. Relationship between First-Order Decay Coefficients in Ponds, for Plug Flow, CSTR and Dispersed Flow Regimes. *Water Sci. Technol.* **2002**, *45*, 17–24. [CrossRef]
40. Gatidou, G.; Oursouzidou, M.; Stefanatou, A.; Stasinakis, A.S. Removal Mechanisms of Benzotriazoles in Duckweed Lemna Minor Wastewater Treatment Systems. *Sci. Total Environ.* **2017**, *596–597*, 12–17. [CrossRef] [PubMed]
41. Ekperusi, A.O.; Nwachukwu, E.O.; Sikoki, F.D. Assessing and Modelling the Efficacy of Lemna Paucicostata for the Phytoremediation of Petroleum Hydrocarbons in Crude Oil-Contaminated Wetlands. *Sci. Rep.* **2020**, *10*, 8489. [CrossRef] [PubMed]
42. Muthusaravanan, S.; Sivarajasekar, N.; Vivek, J.S.; Paramasivan, T.; Naushad, M.; Prakashmaran, J.; Gayathri, V.; Al-Duaij, O.K. Phytoremediation of Heavy Metals: Mechanisms, Methods and Enhancements. *Environ. Chem. Lett.* **2018**, *16*, 1339–1359. [CrossRef]
43. Leitenmaier, B.; Küpper, H. Compartmentation and Complexation of Metals in Hyperaccumulator Plants. *Front. Plant Sci.* **2013**, *4*, 374. [CrossRef] [PubMed]
44. Correia, R.R.S.; de Oliveira, D.C.M.; Guimarães, J.R.D. Total Mercury Distribution and Volatilization in Microcosms with and Without the Aquatic Macrophyte Eichhornia Crassipes. *Aquat. Geochem.* **2012**, *18*, 421–432. [CrossRef]

45. Sundaramoorthy, P.; Chidambaram, A.; Ganesh, K.S.; Unnikannan, P.; Baskaran, L. Chromium Stress in Paddy: (i) Nutrient Status of Paddy under Chromium Stress; (ii) Phytoremediation of Chromium by Aquatic and Terrestrial Weeds. *Comptes Rendus Biol.* **2010**, *333*, 597–607. [CrossRef]
46. Pelcová, P.; Kopp, R.; Ridošková, A.; Grmela, J.; Štěrbová, D. Evaluation of Mercury Bioavailability and Phytoaccumulation by Means of a DGT Technique and of Submerged Aquatic Plants in an Aquatic Ecosystem Situated in the Vicinity of a Cinnabar Mine. *Chemosphere* **2022**, *288*, 132545. [CrossRef]